ELSEVIER

Journal of Structural Geology 27 (2005) 1027–1045

JOURNAL OF STRUCTURAL GEOLOGY

www.elsevier.com/locate/jsg

The use of porphyroblasts to resolve the history of macro-scale structures: an example from the Robertson River Metamorphics, North-Eastern Australia

M. Cihan*, A. Parsons

School of Earth Sciences, James Cook University, Townsville, Qld 4814, Australia

Received 23 June 2004; received in revised form 11 February 2005; accepted 14 February 2005
Available online 6 June 2005

Abstract

The successions of inclusion trail asymmetries defining foliation intersection/inflection axes (FIAs) preserved in porphyroblasts document the geometry of deformation associated with folding and fabric development during discrete episodes of bulk shortening and suggest that deformation histories are commonly more complex than previously considered. A succession of four FIAs trending ENE–WSW, E–W, N–S and NE–SW has been distinguished based upon relative timing plus inclusion texture and orientation in the Proterozoic Robertson River Metamorphics (Georgetown Inlier, Qld, Australia). The successions of asymmetries formed around these FIAs bear no relationship to the geometry of macroscale folds present in the area suggesting that these folds predate porphyroblast growth, the widespread metamorphism and matrix fabric development. The onset of regional macro-scale folding may have begun soon after the deposition at around 1655 Ma in the Georgetown Inlier as opposed to the previously suggested date of 1570 Ma. These folds were then amplified, overturned and refolded during NNW–SSE, N–S, E–W and NW–SE directed regional bulk shortening. Earlier deformations were erased from the matrix because of bedding-induced shearing (reactivation) on the limbs of pre-existing macro-scale folds. Four foliations, S_1–S_4, identified in the matrix provided information about the youngest deformations preserved in these rocks. These results also suggest that existing tectonothermal models regarding the NE Australian Craton should be reconsidered.

Keywords: Georgetown Inlier; Robertson River Metamorphics; Foliation intersection/inflection axes (FIA); Porphyroblasts; Inclusion trails; Deformation partitioning

1. Introduction

Solving the relationships between matrix foliations and those preserved in porphyroblasts in highly tectonized terrains is vital for the development of a complete understanding of the deformation and metamorphic history and has been highlighted in numerous studies (e.g. Zwart, 1960; Vernon, 1978, 1989; Williams, 1985, 1994; Paterson and Vernon, 2001). However, a new quantitative technique including the analysis of inclusion trails in 3D (e.g. Bell et al., 2003 and references therein) has resulted in insights that challenge these earlier approaches. This technique enables the measurement of foliation intersection/inflection axes (FIAs) preserved within the porphyroblasts that have resulted from the overprinting of successively formed foliations (e.g. Bell et al., 1995) or the rotation of porphyroblasts (e.g. Rosenfeld, 1970). The FIA method is completely independent of whether porphyroblasts rotate or not and enables one to test rotation versus non-rotation models. If the porphyroblasts have rotated, the FIA represent the rotation axis and reveal the main direction of shearing or tectonic transport in an area (Rosenfeld, 1970; Schonefeld, 1979). If they have not rotated, the FIA lie perpendicular to the direction of bulk shortening that caused orogenesis (e.g. Bell et al., 1995).

Inclusion trails in porphyroblasts commonly provide information about early deformation events that are obliterated from the matrix. Porphyroblasts are generally more competent than the matrix and preserve early-formed foliations from the effects of younger deformation and

* Corresponding author. Tel.: +61 7 4781 6810; fax: +61 7 4725 1501.
E-mail address: mustafa.cihan@jcu.edu.au (M. Cihan).

0191-8141/$ - see front matter © 2005 Elsevier Ltd. All rights reserved.
doi:10.1016/j.jsg.2005.02.004

metamorphism. In the matrix these foliations are destroyed or rotated towards the compositional layering due to reactivation and shearing along S_0 (Bell et al., 2003). Consequently, the matrix foliations provide information on only the very youngest deformation events (e.g. Hickey and Bell, 2001). Measurement of FIAs and associated inclusion trails asymmetries can potentially supply useful information on the timing and mechanism of development of regional folds (e.g. Visser and Mancktelow, 1992; Stallard and Hickey, 2001). They also allow correlation of the orogenic history across large regions (Bell et al., 2004) and determination of P–T paths that have been obliterated elsewhere in the rock. These approaches have been applied in the Robertson River Metamorphics, Georgetown Inlier, which is an important metamorphic terrain that preserves a prolonged Proterozoic tectono-metamorphic history in northeast Australia.

2. Geological setting

The Georgetown Inlier contains one of the most extensive exposures of Precambrian rocks in north Queensland, Australia (Fig. 1). Other Precambrian inliers, the Coen, Yambo, Woolgar and Mount Isa, are separated from the Georgetown Inlier and one another by Phanerozoic rocks, and have been related to one another based on deformational pattern and isotopic ages (Withnall, 1996; Black et al., 1998). These inliers formed as back arc basins within intermittently extending continental crust in the overriding plate of a subduction system between 1800 and 1670 Ma (e.g. Giles et al., 2002). There has been some controversy over whether the first deformation involved N–S shortening followed by younger deformation events accompanying E–W directed shortening (Bell, 1983) or was the result of progressive thin-skinned westward thrusting was followed by thick-skinned E–W shortening involving the formation of N–S-trending folds (MacCready et al., 1998; Betts et al., 2002).

The study area (Fig. 2) contains intrusive rocks such as the Carboniferous–Permian rhyolite, dacite and microgranite, the Proterozoic Cobbolt Metadolerite and Digger Creek Granite, as well as the Proterozoic Robertson River Metamorphics (White, 1965). The latter rocks include six highly deformed units ranging from low metamorphic grade in the east to high in the west. These units have been named the Lane Creek and Corbett Formations, Thin Hill Quartzite Member, Dead Horse Metabasalt, Daniel Creek Formation and Mount Helpman Member and consist of highly deformed phyllite, pelitic schist, amphibolites, quartzites and rare calc-silicate gneiss (Withnall, 1985). Based on the absolute dating of intrusive rocks bounding the top and bottom of these units, the depositional age lies between 1695.8 ± 1.5 and 1655 ± 2.2 Ma (Black et al., 1998). Previous studies (Black et al., 1979; Bell and Rubenach, 1983) proposed two major tectonothermal events for the Proterozoic Georgetown Inlier. These were dated as D_1 1570 ± 20 Ma and D_2 1553 ± 3 Ma (Black et al., 1979, 1998). The next four deformations were associated with local crenulations during retrogressive metamorphism.

3. Methods

Fieldwork involved the measurement of matrix foliations and lineations and the collection of 68 oriented samples from the staurolite and sillimanite zones (Fig. 2) in which well-developed porphyroblasts are present. For each rock sample, six vertical thin sections were cut in 30° increments around the compass to determine the geometry of the structures in 3D (Cihan, 2004). Inclusion trails within staurolite and garnet porphyroblasts were examined in each thin section together with matrix foliations. Extra thin sections at 10° intervals were cut between the two sections where the asymmetry (clockwise or anticlockwise) of curvature of single or overprinting inclusion trails switched. The FIA was determined as lying between the 10° sections where the asymmetry flips (e.g. Bell et al., 1995). FIAs were measured for each oriented rock sample relative to both geographic coordinates and the normal to the earth surface. Multiple FIA trends were distinguished in some samples using changes in trend from core to rim as well as from early garnet to younger staurolite porphyroblasts.

4. Deformation events

Evidence for multiple deformations was observed micro- and macroscopically. Structures associated with successive deformation events in the matrix were correlated from sample to sample and outcrop to outcrop using consistency in the orientation and the overprinting succession of folds, foliations and crenulations, and four deformations were differentiated. However, detailed analysis of microstructures trapped in porphyroblasts suggests that there were several deformation events that preceded the ones preserved in the matrix.

4.1. Deformation events recorded in the matrix

Four generations of foliation, S_1, S_2, S_3 and S_4, preserved in the matrix throughout the study area. S_0, in the porphyroblastic schists, is characterized by mm to cm scale compositional layering that has resulted from a changing grain size, colour and minerals from one layer to another. The stereonet plot of poles to S_0 suggests they are folded about an approximately NNW-trending axes (Fig. 3) on a smaller scale than the larger scale ENE–WSW- and E–W-trending fold outlined by mappable compositional layering such as the Dead Horse Metabasalt and Cobbold Metadolerite (Fig. 2). The latter structures are west plunging and consist of a tight to moderate overturned anticline and

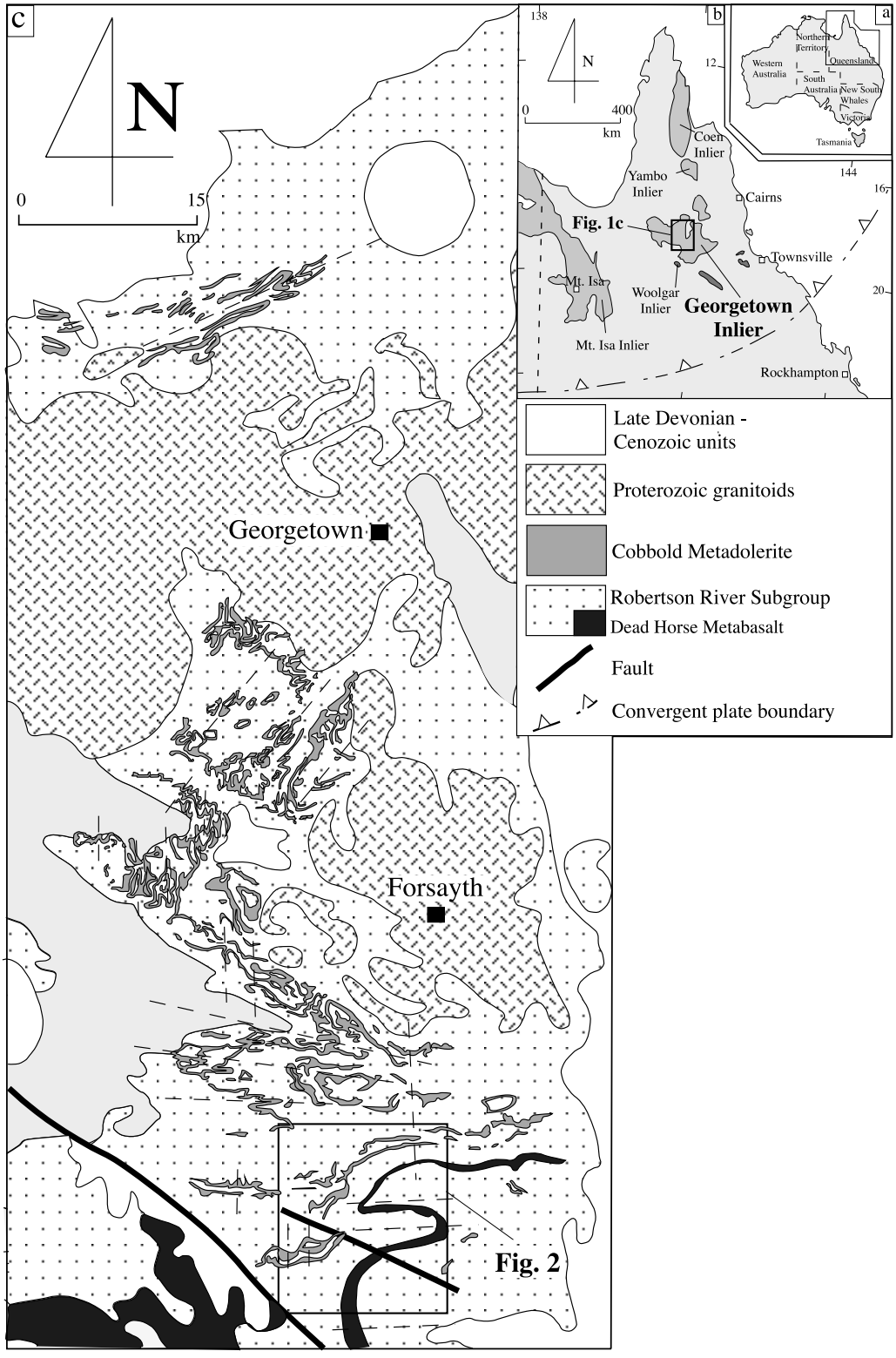

Fig. 1. Location map showing the major regional geological features of the central Georgetown Inlier, North Queensland, Australia. The inset box highlights the area in which detailed study was performed (compiled from Withnall (1985) and Bain et al. (1985)).

syncline (F_{1-2}; Figs. 1 and 2). They seem to have been refolded around the N–S-trending folds (F_3; Fig. 2). S_1 is preserved in zones where the dominant foliation is less intensely developed as a crenulated cleavage or an inclusion trail (Figs. 4 and 5a and b). The dominant foliation represents rotated S_1 towards the compositional layering because of reactivation of S_0 during D_2 (e.g. Bell et al., 2003). During this process, for instance, progressive dextral

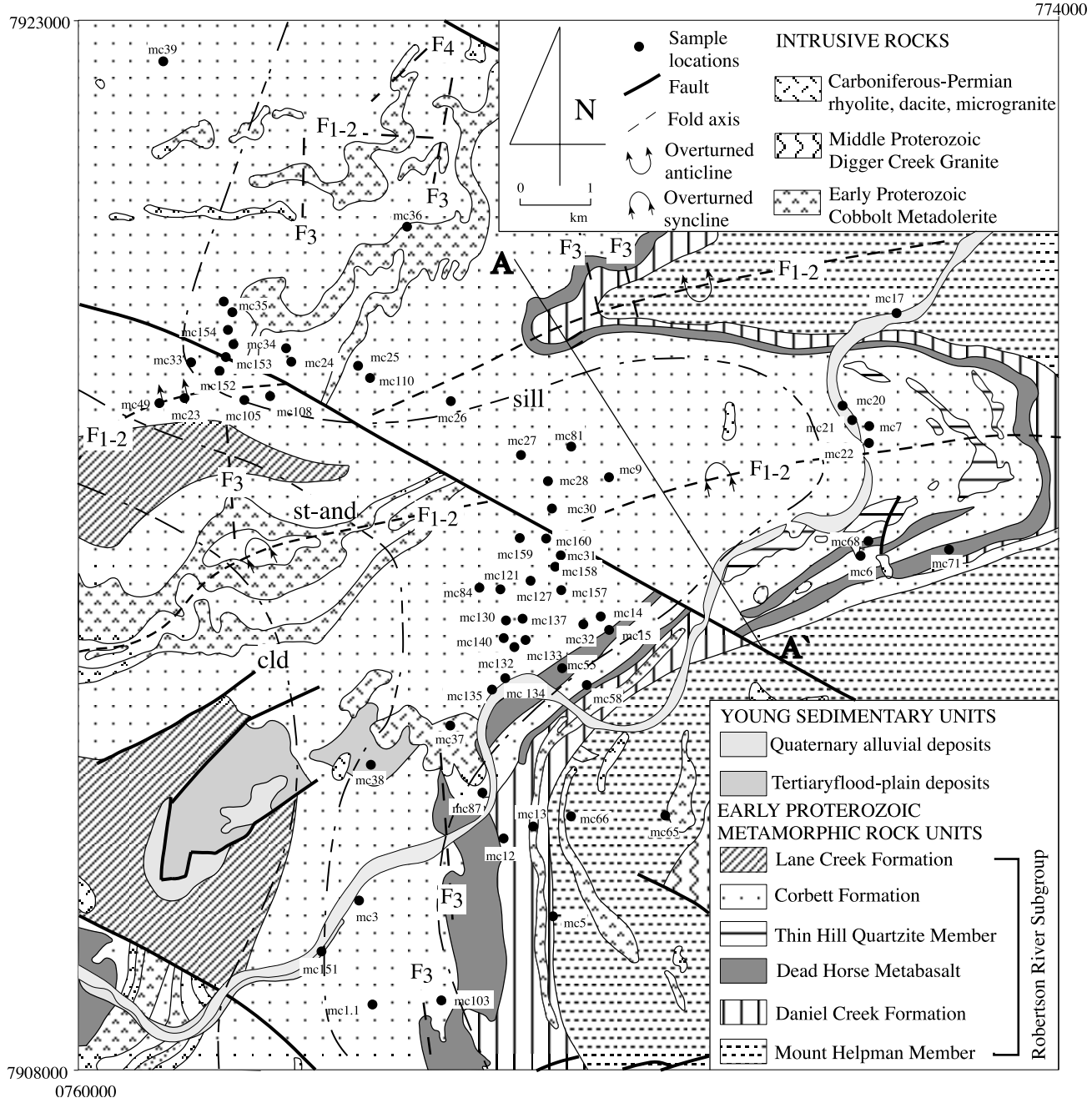

Fig. 2. Detailed geological map of the study area outlined in Fig. 1c (modified from Bain et al. (1985)). The folded dash lines, which crosscut the lithologic trends, represent the sillimanite (sill), staurolite–andalusite (st–and), chloritoid (cld) isograds. A–A' line shows the position of the cross-section in Fig. 12.

shearing acting along S_2 switched to sinistral shearing along the compositional layering and S_2 was destroyed whilst S_1 was decrenulated and rotated towards the compositional layering in the matrix (Fig. 5c and d). Consequently, the dominant foliation is neither S_1 nor S_2. It is called $S_{1/2}$ from now on. $S_{1/2}$ is mainly E–W-trending, north dipping, and folded around N–S-trending axes. The intersection lineation ($L^0_{1/2}$) and the stretching lineation ($L^{1/2}_{1/2}$; Fig. 6) lies in the northern quadrants of the stereonet around the N–S axis suggests these might have been distributed on the limbs of N–S folding. S_2 is preserved locally as a differentiated crenulation cleavage in porphyroblast strain shadows or as inclusion trails (Fig. 7). N–S folds suggest that it might have been originally formed as a ~N–S-trending steeply dipping foliation parallel to axial plane of these folds (Fig. 2). S_3 is a gently dipping weakly developed crenulation (Fig. 4) that locally intensifies to schistosity (Fig. 7). The stereonet plot of poles suggests that S_3 is mainly NNW-trending and NE dipping but it is also folded about an axis plunging towards the NNE (Fig. 8). The intersection lineation, $L^{1/2}_3$, spreads in the NW and NE quadrants of the stereonet probably because of the folding of S_3 planes with low amplitudes. S_4 has

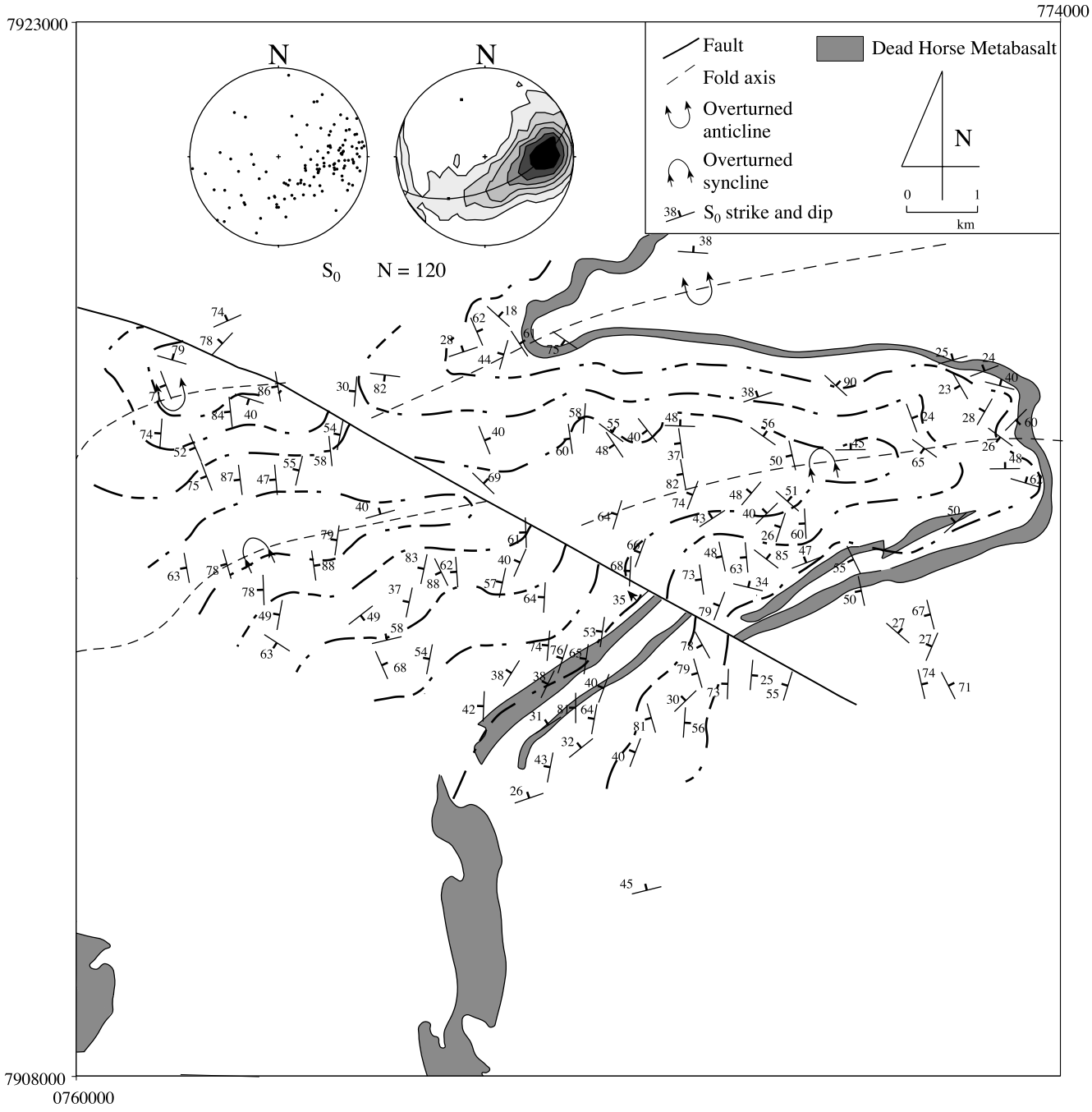

Fig. 3. A structural map of bedding (S_0) orientations and form-line trends. Note that in plan view, form lines lie parallel to the limbs of macroscopic folds outlined by the Dead Horse Metabasalt. Although these folds have ~E–W axial traces, stereonet plots suggest that S_0 is folded around NNW–SSE trending axes.

developed parallel to the axial plane of these folds as the steeply dipping axial plane of crenulations (Figs. 7 and 8) striking mainly towards the NNE and $L_4^{1/2}$ lies more consistently in the NE quadrant. The comparison of matrix foliations with respect to the limbs of the ENE–WSW- and E–W-trending folds (F_{1-2}) indicates that $S_{1/2}$ and S_3 are shallower and S_4 steeper than the limbs of these folds (Fig. 9). This suggests that these macro-scale folds were formed potentially much earlier than the currently visible matrix foliations. If this was the case, there must have been earlier deformations that have been obliterated from the matrix because of subsequent reactivation (Bell et al., 2003).

4.2. Deformation events recorded in porphyroblasts

Foliations that are no longer preserved within the matrix were trapped in garnet, staurolite, biotite, plagioclase,

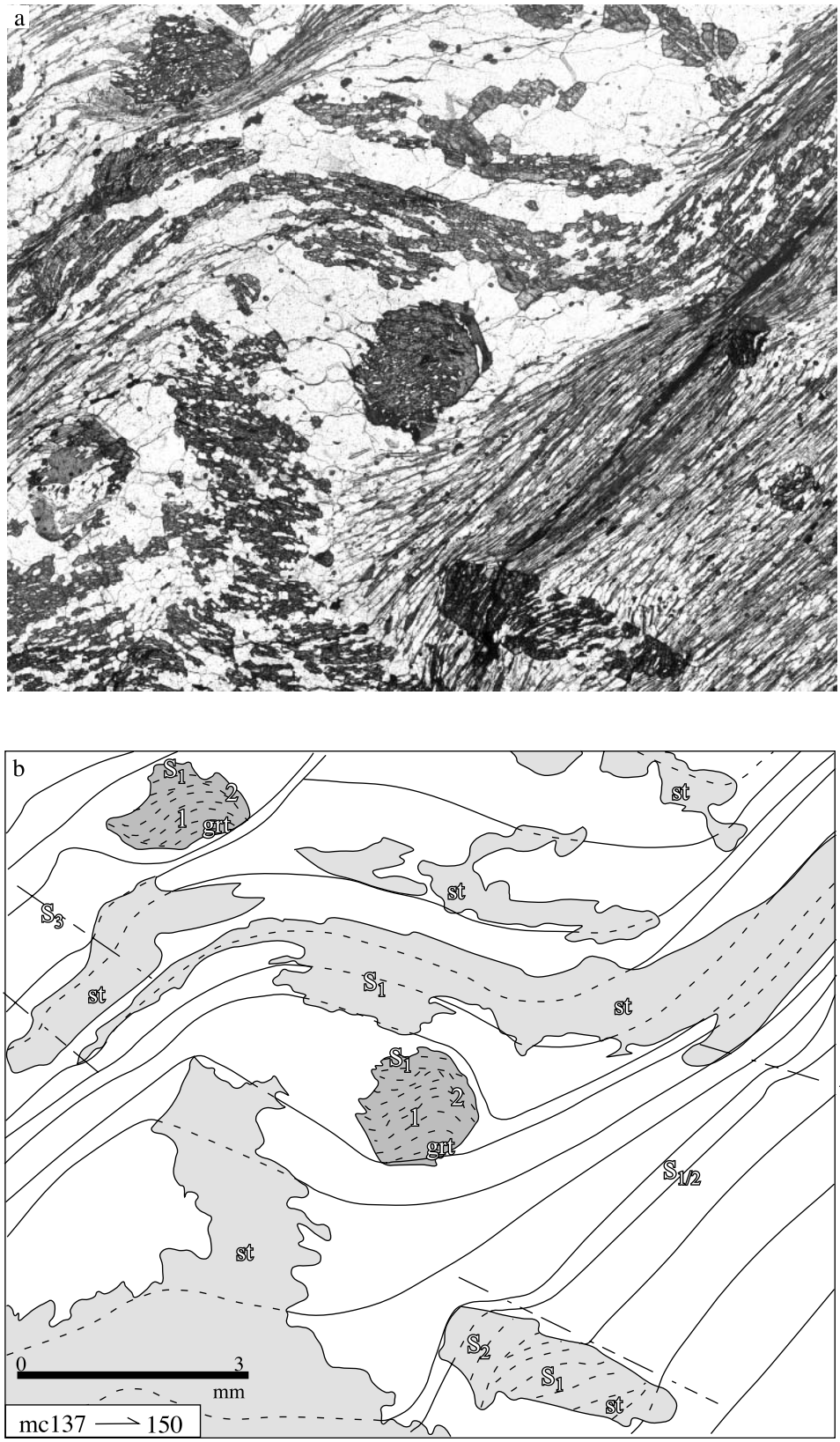

Fig. 4. Photomicrograph from a vertical thin section shows garnet (grt) wrapped by a staurolite (st) porphyroblast (a). As shown in interpreted line diagram (b), two pre-matrix foliations were overgrown by garnet porphyroblast whereas staurolite porphyroblast overgrew S_1 and $S_{1/2}$ as represented by a crenulation hinge and the dominant matrix foliation in the matrix, respectively. S_3 is a weak crenulation.

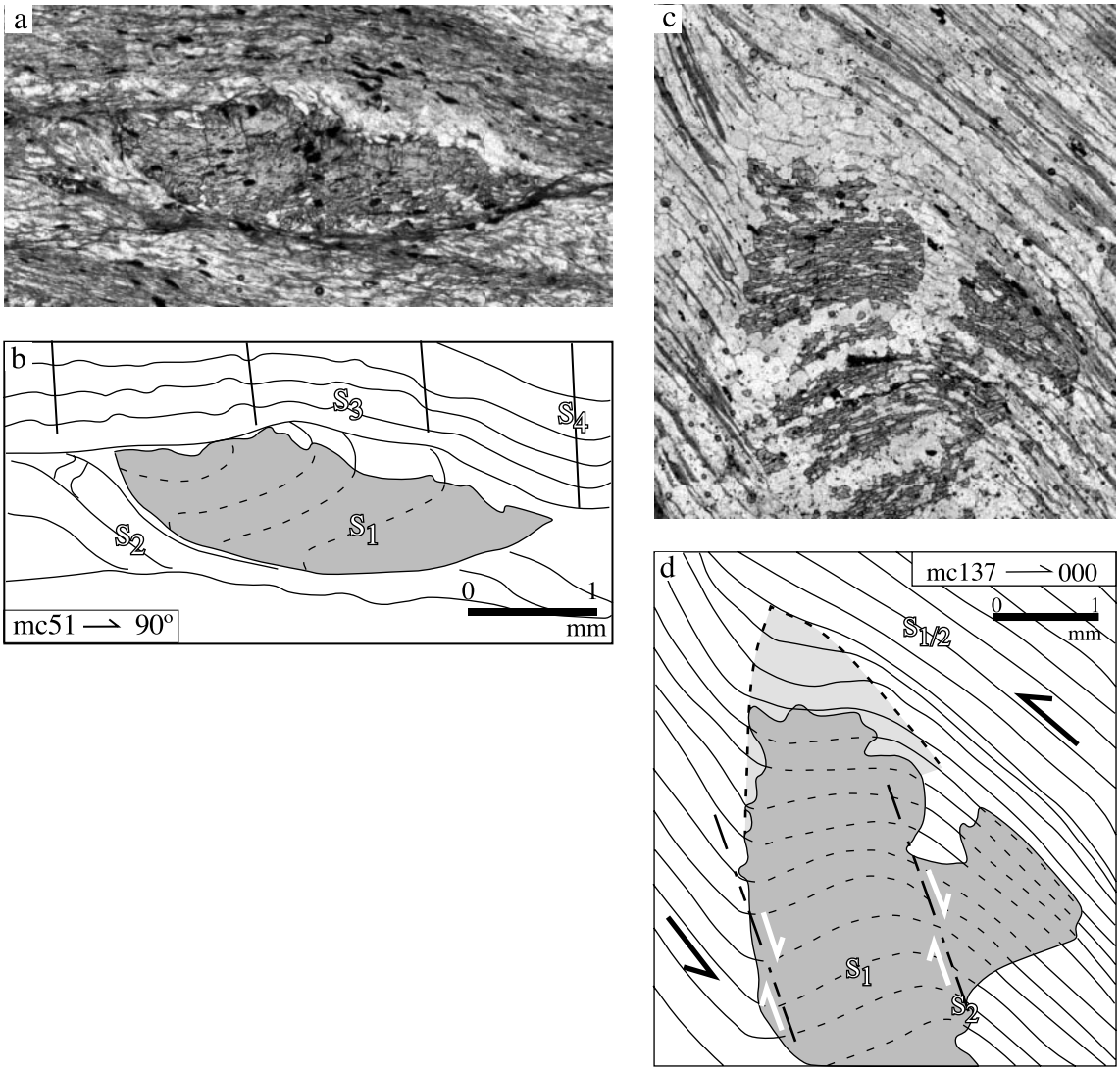

Fig. 5. Photomicrographs from vertical thin sections show a chloritoid (a) and a staurolite (c) porphyroblasts with sigmoidal type inclusions, which represent low- and higher-grade of the Robertson River Metamorphics, respectively. Both interpreted line diagrams ((b) and (d)) displays different generation of foliations. Line diagram in (d) depicts the reactivation of the earlier foliation (S_1) in the matrix (c). S_1 is trapped within the staurolite as a hinge of a differentiated crenulation cleavage (S_2). Light barbed arrows represent the clockwise sense of shear on the steep S_2 foliation formed at the beginning of D_2. D_2 Q-domain (shaded with light grey) was destroyed in the matrix with anticlockwise shear sense (black barbed arrows) and S_1 was decrenulated and rotated to form a composite schistosity ($S_{1/2}$).

chloritoid and andalusite porphyroblasts as inclusion trails. Garnet and staurolite porphyroblasts were especially useful since they are abundant in most rock samples and contain well-preserved inclusion trails consisting of elongated quartz, ilmenite, epidote and rarely biotite. In garnet porphyroblasts these trails usually have sigmoidal geometries defining microfold hinges (Figs. 4 and 7a and b), but some samples contain staircase (Fig. 7c and d) and spiral shaped geometries (Fig. 10). The matrix foliation usually truncates the inclusions in garnet porphyroblasts, but it is also possible to observe textural discontinuities between core and rim inclusion trails (Figs. 4, 7 and 10; Cihan, 2004). Staurolite porphyroblasts commonly contain garnet porphyroblasts as inclusions that are wrapped by inclusion trails that are sigmoidal (Fig. 4), straight with curvature at the rim that continues into the matrix, or differentiated crenulations (Figs. 4 and 11). The continuity of inclusions enables correlation between different growth phases of staurolite porphyroblasts versus development of the matrix foliations (Figs. 4 and 11). Based on these relationships, staurolite porphyroblasts overgrew successively formed S_1, S_2 and S_3 foliations that are usually observed as the hinges of crenulations or parallel to the matrix (Figs. 4 and 5c and d). In lower grade areas (Cld isograd in Fig. 2), chloritoid contain S_1 as sigmoidal type inclusion trails (Fig. 5a and b), which can be correlated with staurolite porphyroblasts (Fig. 5c and d) in upper grade areas towards east (st–and isograd in Fig. 2). Pre-S_1 foliations could only be correlated and characterized based on FIAs since they are truncated by the matrix foliations.

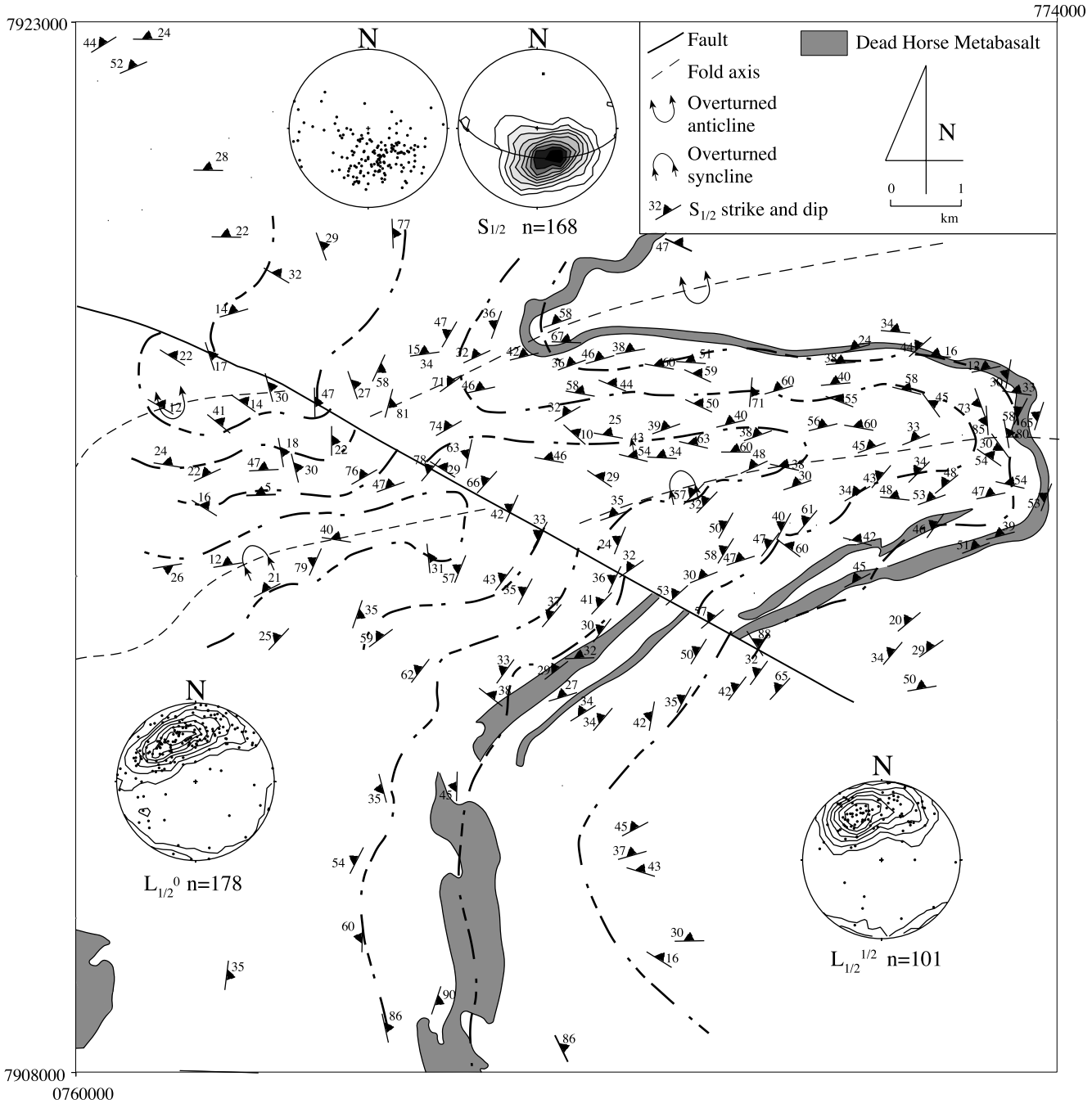

Fig. 6. A structural map of the $S_{1/2}$ dominant foliation and interpreted $S_{1/2}$ form-lines. A stereonet plot of $S_{1/2}$ suggests folding around N–S-axes. Stereonet plots of stretching lineations ($L^{1/2}_{1/2}$) and intersection lineations ($L^{0}_{1/2}$) indicate the distribution of these on the limbs of N–S folds (F_3).

A total of 112 FIAs were measured from successively formed foliations trapped as inclusion trails in garnet and staurolite porphyroblasts in the rock samples (Fig. 2). Four FIAs (Fig. 12) were determined (Cihan, 2004) and these are tabulated with respect to individual samples in Table 1 and their trends are plotted on rose diagrams (Fig. 13).

The earliest formed FIA (FIA1) trends approximately ENE–WSW and is found in the cores of the garnet porphyroblasts. FIA2 occurs in an E–W orientation and in the core and the rims of garnet porphyroblasts. It is also present in some samples within staurolite porphyroblasts (Fig. 14a and b). The FIA3 is N–S-trending and is equally distributed between porphyroblast phases as the dominant trend (Fig. 14a and b). FIA4, trending between 30° and 50°N, is only visible in staurolite porphyroblasts (Fig. 14c). FIA1 (ENE–WSW) and FIA2 (E–W) are described by pre-S_1 foliations whereas FIA3 (N–S) and FIA4 (NE–SW) are typified by $S_{1–2}$ and $S_{3–4}$, respectively, which are rotated

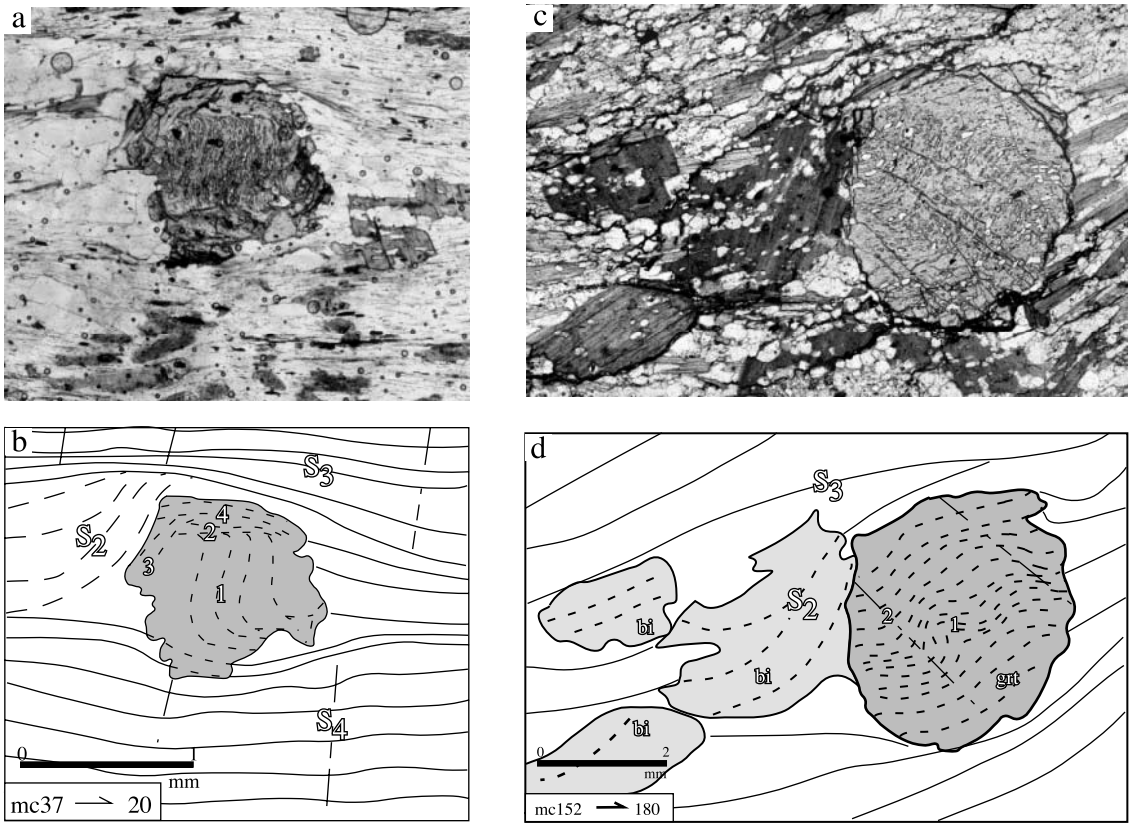

Fig. 7. Photomicrograph from a vertical thin section shows a garnet porphyroblast with a complex inclusion pattern (a). A line diagram shows the interpretation of successively formed foliations and textural discontinuities both in the porphyroblast and in the matrix (b). The numbers 1–4 represent different groups of pre-existing foliations trapped within the porphyroblast. S_2–S_4 represent the foliations identified in the matrix. Another photomicrograph from a vertical thin section shows a garnet porphyroblast with staircase inclusion trails (c). Interpreted line diagram (d) depicts a pre-existing foliation (1) and crenulation cleavage (2). S_2 is a steeply dipping foliation in biotite (bi) porphyroblast formed in the strain shadow of the garnet (grt) porphyroblast. S_3 is a gently dipping foliation intensified towards compositional layering.

towards main schistosity in the matrix. Significantly, the FIA1 and FIA2 trends are consistent with E–W folds (F_{1-2}), whereas FIA3 and FIA4 are consistent with N–S (F_3) and NE–SW (F_4) folds in a larger area (Fig. 1c) including the Robertson River Metamorphics (Fig. 2). These FIA trends appear to have formed perpendicular to the bulk shortening directions, which changed from NNW–SSE to N–S to E–W and finally to NW–SE as orogenesis continued.

Although sigmoidal and spiral inclusion trails have been interpreted as having formed by porphyroblast rotation (e.g. Rosenfeld, 1970), the preservation of a succession of four different FIAs with consistent trends requires that the earlier formed porphyroblasts were not rotated during development of the younger formed ones (Cihan, 2004). It is argued that if refolding of the early-formed FIA trends had occurred or the porphyroblasts had rotated, then a whole range of different FIAs should have been observed with erratic relative timing. Consequently, this data set suggests non-rotational porphyroblast growth over at least four different periods in the area investigated.

5. The implications of inclusion trail asymmetries and FIA orientations for macro-scale folding

The curvature of inclusion trails in porphyroblasts preserves the asymmetry of a crenulation cleavage as it passes into the younger differentiated crenulation cleavage (Bell et al., 2003). This asymmetry should change across any fold hinge that the porphyroblasts grew synchronously with. For example, for an antiform, the differentiation asymmetry that formed as the fold developed should switch from anticlockwise on the northern limb to clockwise on the central limb looking west with sinistral to dextral shear senses, respectively, as shown in Fig. 14a. For a synform it is the opposite (Fig. 14a). Although matrix differentiation asymmetries are routinely obliterated by younger deformation, the history of differentiation asymmetry that can potentially be related to fold development is commonly trapped within porphyroblasts (Bell et al., 2003). Differentiation asymmetries are determined while examining sections orthogonal to successive FIA sets. They can be presented as histograms (Fig. 14b) separated according to limb on the E–W-trending folds. On these histograms, each

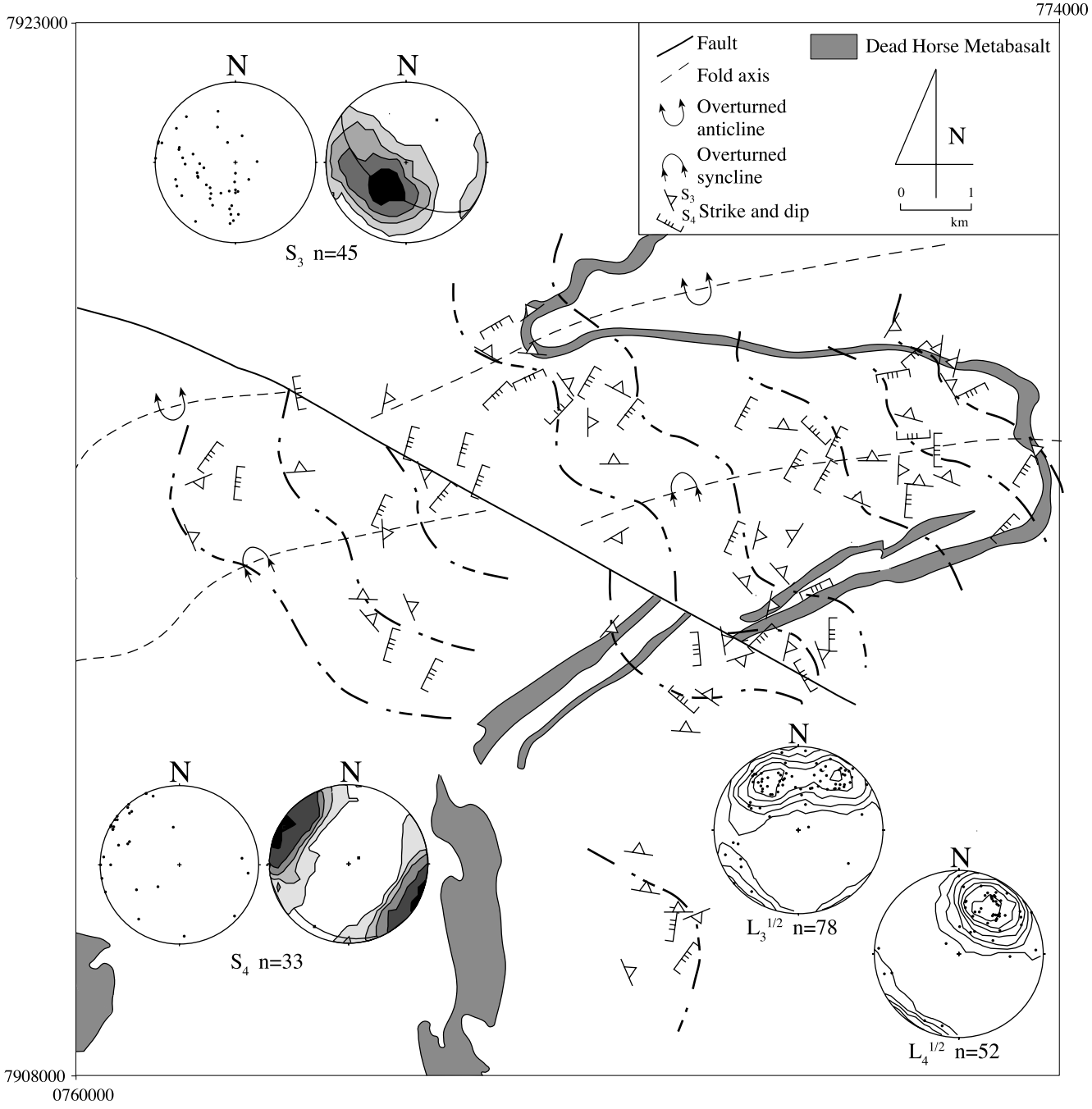

Fig. 8. A structural map of S_3 and interpreted form-lines. Stereonet plot of S_3 suggests folding around a NE–SW axis. $L_3^{1/2}$ lineations are distributed in northern quadrants and $L_4^{1/2}$ lineations lie parallel to the axial plane of NE–SW folds (F_4).

box includes clockwise (CW) or anticlockwise (ACW) asymmetries observed for each FIA trend. For FIA1 (ENE–WSW) the asymmetry is predominantly clockwise on the northern limbs of the two antiforms (A and C in Fig. 14b) for both sub-horizontal and sub-vertical events, which represents successively formed gently and steeply dipping generations of foliation. These asymmetries are the opposite of those expected for these limbs of the folds and hence the fold did not form during the development of FIA1 (ENE–WSW). The asymmetries for FIA2 (E–W) in the northernmost limb are mostly clockwise for predominantly sub-horizontal events. In the central limb, they are also predominantly clockwise for sub-horizontal foliation producing events. In the southernmost limb clockwise and anticlockwise asymmetries are equally present but clockwise asymmetries for sub-horizontal events prevail. The asymmetries for FIA3 (N–S) are primarily clockwise throughout the folds and sub-horizontal foliation producing events are dominant. However, FIA3 (N–S) is perpendicular to axial plane of these folds and since the asymmetries are

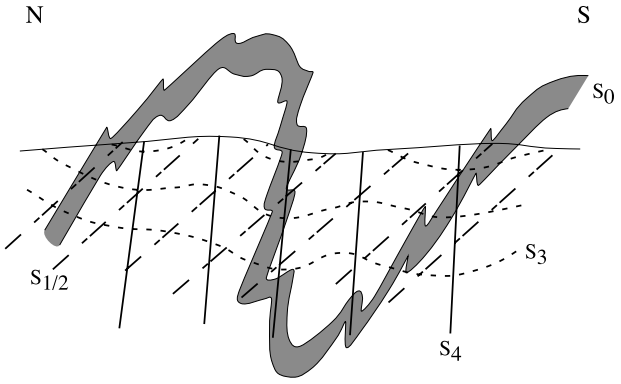

Fig. 9. A simplified cross-section taken along a line A–A′ in Fig. 2 shows the relationships of matrix foliations with respect to macro-scale E–W-trending folds.

viewed in thin sections parallel to the axial plane of E–W folds, they show no relationship to the folds. These asymmetries can only be related to N–S folds in the study area. For FIA4 (NE–SW) the asymmetries accord with those expected for the northern and central limbs. However, they do not accord with those for the southern limb. This could be interpreted to suggest that the northern and central limbs formed during the development of FIA4. However, if this were the case, S_4 would not overprint both limbs of this fold with the same vergence asymmetry (Fig. 9). The distribution of porphyroblast growth during the development of FIA4 (NE–SW), as shown in Fig. 12d, suggests that reactivation may have resulted in less porphyroblast growth and/or deformation was not partitioned through the northern and central limbs. Likewise, FIA1 (ENE–WSW) and FIA2 (E–W) porphyroblasts might have been dissolved more, or grown less than the southern limb because of the higher degree of reactivation through this portion (Northern and central limbs in Figs. 12 and 14b and c) of the Robertson River Metamorphics.

6. Discussion

6.1. Reactivation and rotation of early-formed foliations

During reactivation, progressive synthetic shearing occurring along anastomosing foliations parallel to the axial plane switches to antithetic shearing acting along the bedding or compositional layering (fig. 1 in Bell et al., 2003). This

Table 1
A list of FIA measurements for each sample from core and rim of garnet and staurolite porphyroblasts

Sample number	Garnet core–rim	Staurolite core–rim	Sample number	Garnet core–rim	Staurolite core–rim
Mc1.1	105–	175–	Mc158	175–	45–
Mc1.2	105–		Mc159	15–	
Mc103	35–		Mc160	75–	45–
Mc105	85–175		Mc17	95–175	15–
Mc108	95–		Mc2	105–	
Mc110	155–		Mc20		85–
Mc12	85–	175–	Mc21		85–
Mc121	35–		Mc22		175–
Mc130	55–	175–	Mc23	95–	
Mc132A	85–	15–	Mc24	105–	
Mc132B	65–	175–	Mc24.1	85–175	
Mc133	175–	45–	Mc25	105–	
Mc134	145–	25–	Mc26	175–	
Mc135	125–		Mc27	175–	
Mc137	85–	175–	Mc28	175–	
Mc14.1	25–	175–	Mc3	125–	
Mc14.2	95–	15–	Mc30	85–	45–
Mc140	65–	85–	Mc31	155–	175–
Mc15	5–		Mc32	55–	45–
Mc151	85–		Mc33	115–	
Mc152	65–85	175–45	Mc34	25–	
Mc153	95–		Mc35.1	35–	35–
Mc154	55–		Mc35.2	95–	
Mc157	175–	175–45	Mc36	65–85	
Mc37	85–175	45–	Mc66	85–	
Mc38	55–		Mc68	105–	175–
Mc39	65–85	25–	Mc7	15–	45–
Mc49	65–175		Mc71	85–	
Mc5	55–15	175–45	Mc8	175–	175–
Mc55	85–	15–45	Mc81	175–15	45–
Mc58	65–		Mc84	65–	45–
Mc6	95–	35–	Mc87	55–	
Mc13	175–		Mc9	175–	175–
Mc65	65–				

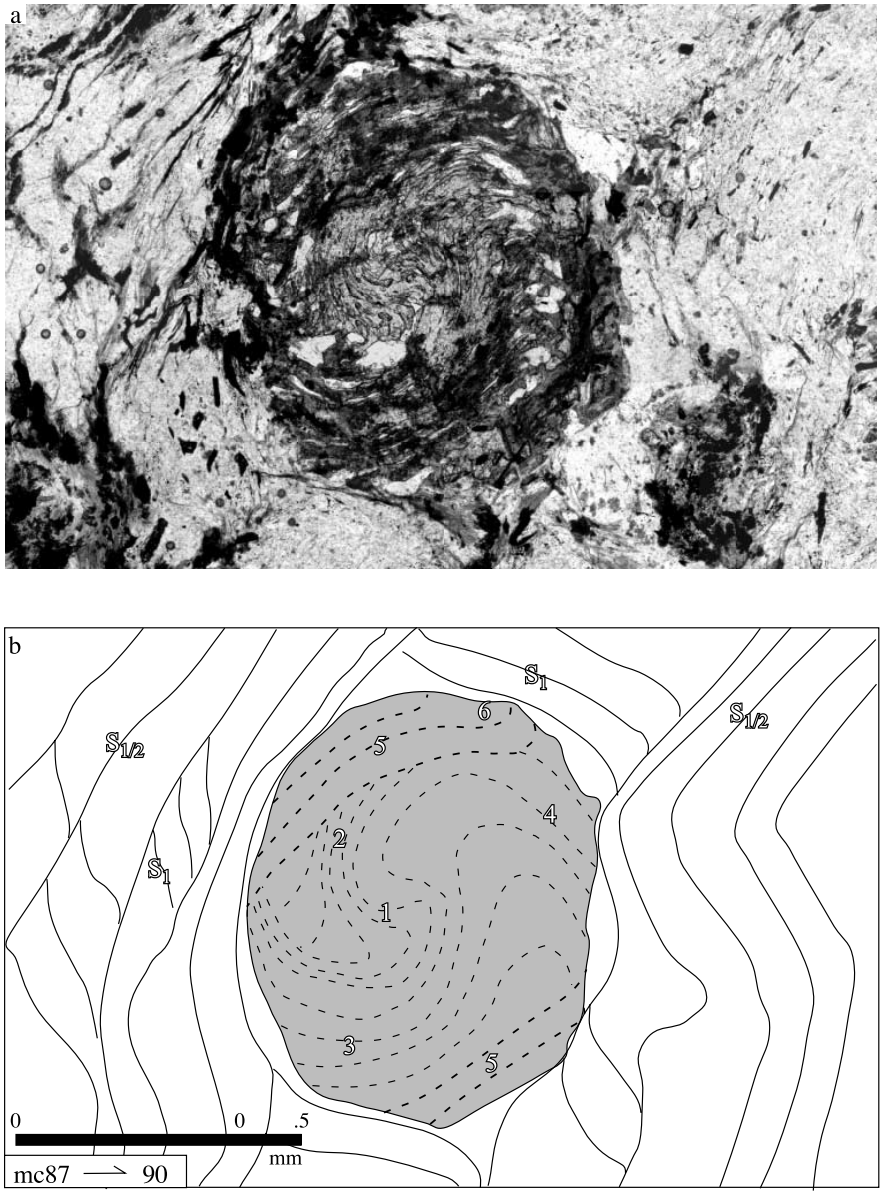

Fig. 10. Photomicrograph from a vertical thin section showing a garnet porphyroblast with spiral inclusion trails truncated by the matrix (a). Accompanying line diagram shows the interpretation of successively formed foliations (1–6), which were trapped as inclusions (b). Truncations of these foliations are visible between inclusion trails exiting the porphyroblast and matrix foliations S_1 and $S_{1/2}$.

causes decrenulation of the older foliation and results in destruction of the developing foliation and rotation of the earlier formed one into parallelism with the compositional layering (Bell, 1986). For this reason, $S_{1/2}$ is commonly observed nearly parallel to compositional layering. It is possible to recognize the effects of reactivation at a range of scales. For example, in Fig. 5c and d, S_1 inclusion trails preserve a D_2 crenulation hinge in a staurolite porphyroblast. S_1 decrenulated and rotated in the matrix and the D_2 Q-domain was destroyed. During this process, originally steep, differentiated S_2 cleavages were destroyed in the matrix. As a result, neither S_1 nor S_2 are preserved as sub-horizontal and sub-vertical foliations in the matrix. The degree of reactivation may change locally based on the competency–contrast differences from one limb of a fold to another or from one layer to another. For instance, it is not possible to see relict S_1 in the matrix in Fig. 5 but in Fig. 10 it is still present; hence reactivation is a heterogeneous process (Bell et al., 1986). Apart from this, the inclusion trails trapped in non-rotated porphyroblasts suggests that it is a key process in erasing the pre-existing foliations from the matrix.

6.2. Porphyroblast growth and deformation partitioning

The character of non-rotational porphyroblasts, including ones containing mainly sigmoidal shaped inclusions (e.g. Figs. 4, 5 and 7) suggest that these preferentially grew

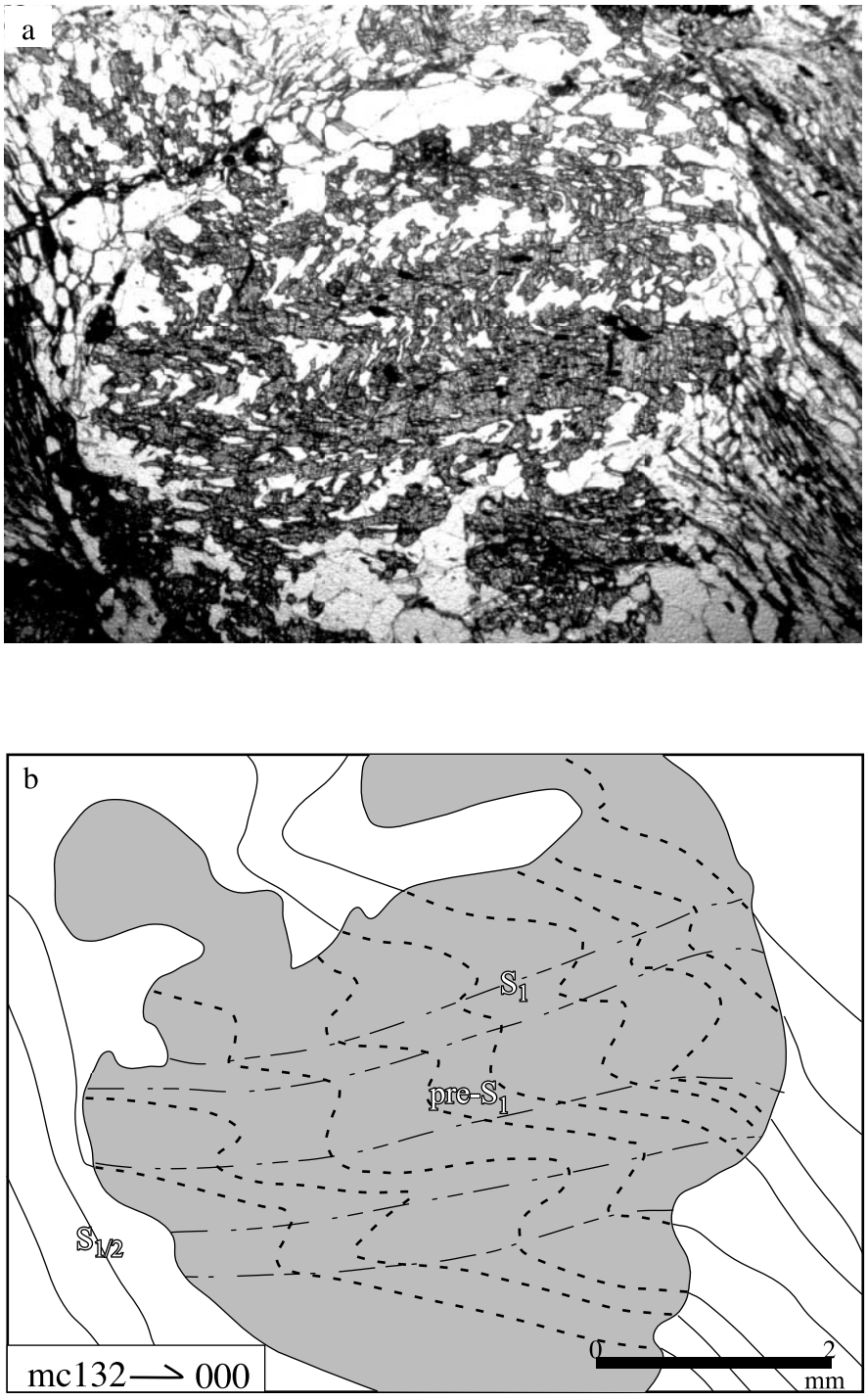

Fig. 11. Photomicrograph from a vertical thin section shows a staurolite porphyroblast preserving a differentiated crenulation cleavage as inclusions (a). Interpreted line diagram (b) shows the differentiated crenulation in which hinges represent gently dipping S_1 and long limb of the crenulations refers to steeply dipping pre-S_1, which is continuous with the matrix foliation $S_{1/2}$.

on crenulation hinges. These sites have been defined as discrete zones of progressive shortening (e.g. Bell et al., 1986; Hayward, 1992; Williams, 1994; Aerden, 1995), whereas the crenulation limbs have been described as progressive shearing domains (e.g. Bell et al., 2004) in which the dissolution of porphyroblasts occurs against mica minerals (e.g. Fig. 5). Growth of porphyroblasts in progressive shortening domains occurs by the aid of microfracturing providing the fluid access needed for the growth reaction to take place (Bell et al., 1986). Such microfracturing happens during the earliest stages of deformation prior to development of a pervasive pattern of deformation partitioning (Fig. 15a–d; e.g. Bell et al., 2004). The domains of deformation partitioning can shift

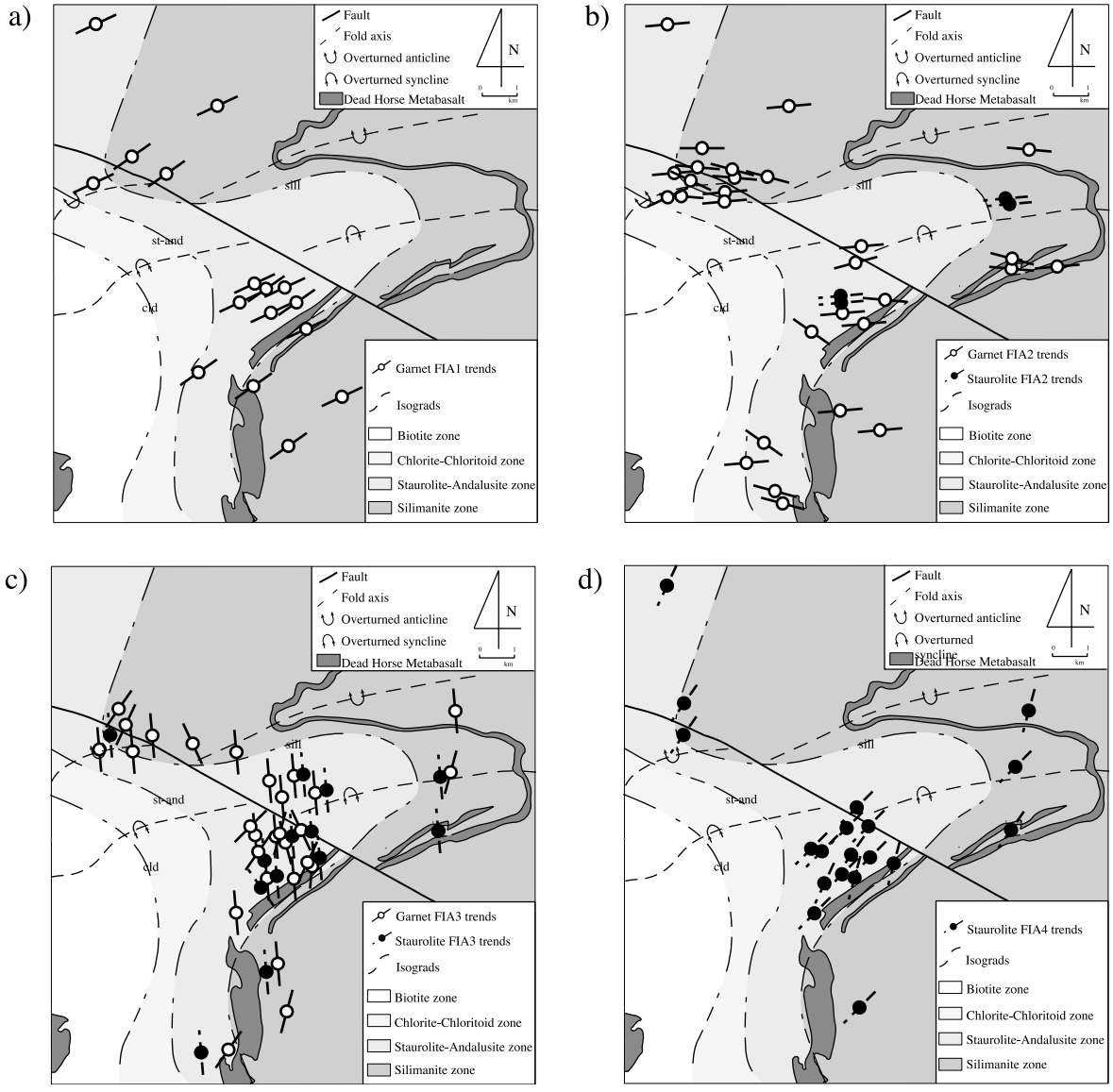

Fig. 12. A map showing the distributions of FIA1 (ENE–WSW), FIA2 (E–W), FIA3 (N–S) and FIA4 (NE–SW) with respect to major structures across the study area.

through the rock as the deformation intensifies or because of younger deformations (Fig. 15e and f). During latter events, either porphyroblasts are completely dissolved or growth may continue on a different fabric, which are new progressive shortening sites formed because of the repartitioning of deformation (Fig. 15f). If additional growth occurs at this stage, FIA trend may change from core to rim depending on the direction of shortening or successively formed foliations may be formed around the same FIA trend (Fig. 10).

The distribution of FIA trends in the study area (Fig. 12) demonstrates the effect of reactivation and deformation partitioning on a macro-scale. The total frequency of porphyroblasts containing FIA1 (ENE–WSW) and FIA2 (E–W) are less than the FIA3 (N–S) porphyroblasts. These first two FIAs were formed by NNW–SSE and N–S shortening, respectively, but FIA3 (N–S) was formed by E–W shortening, which is orthogonal to the earlier directions. In addition, the P–T conditions during the formation of FIA1 (ENE–WSW) to FIA3 (N–S) indicate progressively an increasing clockwise P–T path. This suggests that deformation-partitioning sites should have changed drastically because of the intensity of deformation at the time of formation of FIA3 (N–S). Hence, earlier porphyroblasts were dissolved in significant numbers since they mainly remained in the shearing domains of partitioned deformation. However, an intense degree of reactivation prior to the E–W shortening event could not be excluded since tightening of the fold limbs might have taken up more shearing along compositional layering, especially in the northern and central limbs. Likewise, FIA4 (NE–SW) porphyroblasts formed during NW–SE shortening should

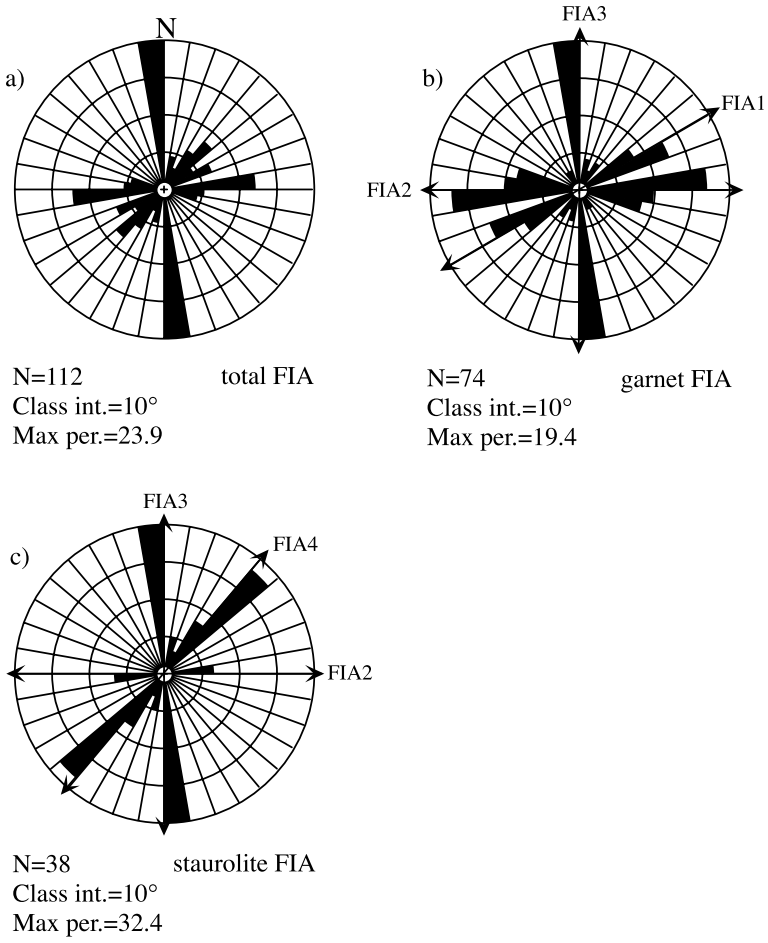

Fig. 13. Rose diagrams showing the orientations of total FIAs (a), FIA1, FIA2 and FIA3 in garnet porphyroblasts (b) and FIA2, FIA3 and FIA4 in staurolite porphyroblasts (c) across the study area.

have grown less in the northern and central limbs in comparison with the southern limb, as readily seen in Fig. 12.

6.3. Evolution of folding events in relation to regional tectonic context

Previously six deformational events were proposed for the Georgetown Inlier (Black et al., 1979; Bell and Rubenach, 1983; Withnall, 1996). The first two major tectonothermal events, D_1 at 1570 ± 20 Ma and D_2 at 1553 ± 3 Ma, were attributed to formation of penetrative foliations associated with prograde metamorphism and the last four produced local crenulations accompanied by retrogressive metamorphism. D_1 was characterized by S_1 foliation that is parallel to the limbs of E–W-trending overturned folds (Bell and Rubenach, 1983; Withnall, 1996). D_2 was distinguished by S_2, which lies parallel to axial planes of NNW–SSE- to N–S-trending folds (Davis, 1996; Withnall, 1996). However, in this study S_1 and S_2 have been distinguished as relic structures in the matrix or within porphyroblasts (Figs. 4 and 5). Thus, what was previously called S_1 and S_2 have been differentiated as the composite fabrics $S_{1/2}$ and S_3, respectively. In addition to these, pre-S_1 structures could not be recognized by earlier studies. These are partly because of the thin sectioning approach that these studies utilized. Cihan (2004) have demonstrated that using multiple vertical thin sections cut around compass reveal much more extensive history than using two thin sections cut with respect to fabric orientations in the matrix (P and N sections). For instance, Bell and Rubenach (1983) using P–N sectioning approach in the same study area suggested that all porphyroblasts overgrew S_1 during D_2 since curving inclusion trails exiting porphyroblasts appeared continuous with the dominant schistosity that they called S_2. However, as also shown here, inclusion trails within garnet porphyroblasts are commonly truncated in the study area. Consequently, these inclusion trails represent the early deformations that were erased from the matrix of a rock and can only be correlated by using FIA trends.

Bell et al. (1995) have argued that consistent successions of FIA trends suggest that the FIAs form orthogonal to the direction of bulk shortening and changes in their trend reflect changes in this direction causing polyphase deformations. The four FIAs shifted from ENE–WSW to E–W to

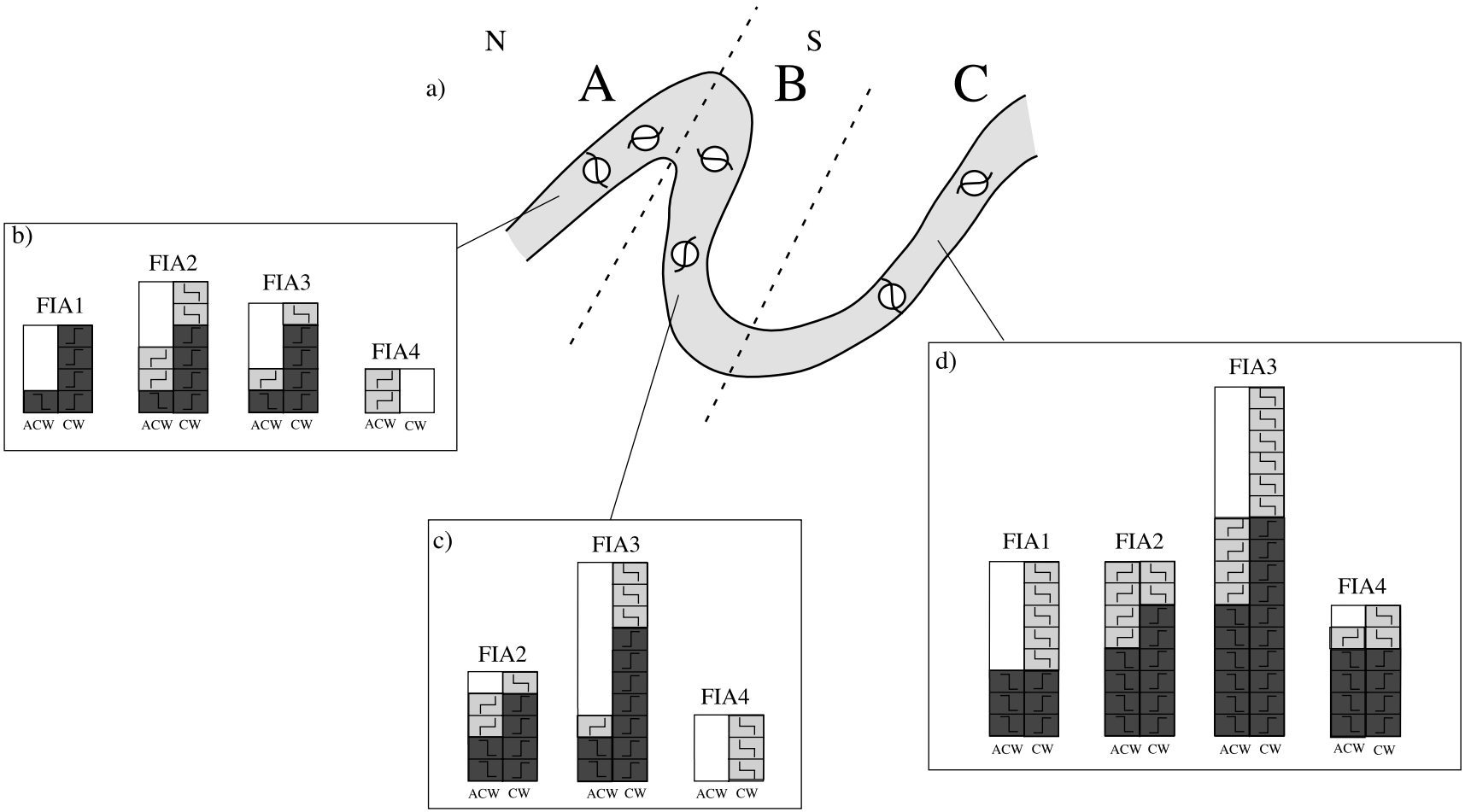

Fig. 14. A sketch cross-section (a) across the folds including both the anticline and syncline in the area. Histograms ((b)–(d)) showing the distributions of asymmetries preserved in porphyroblasts formed around FIA1–FIA4 on the limbs of the folds divided as A, B and C. The S and Z shaped lines on the columns of histograms refer to asymmetries observed for FIAs with top to the left or right, and right side up or down shear senses. ACW, anticlockwise; CW, clockwise.

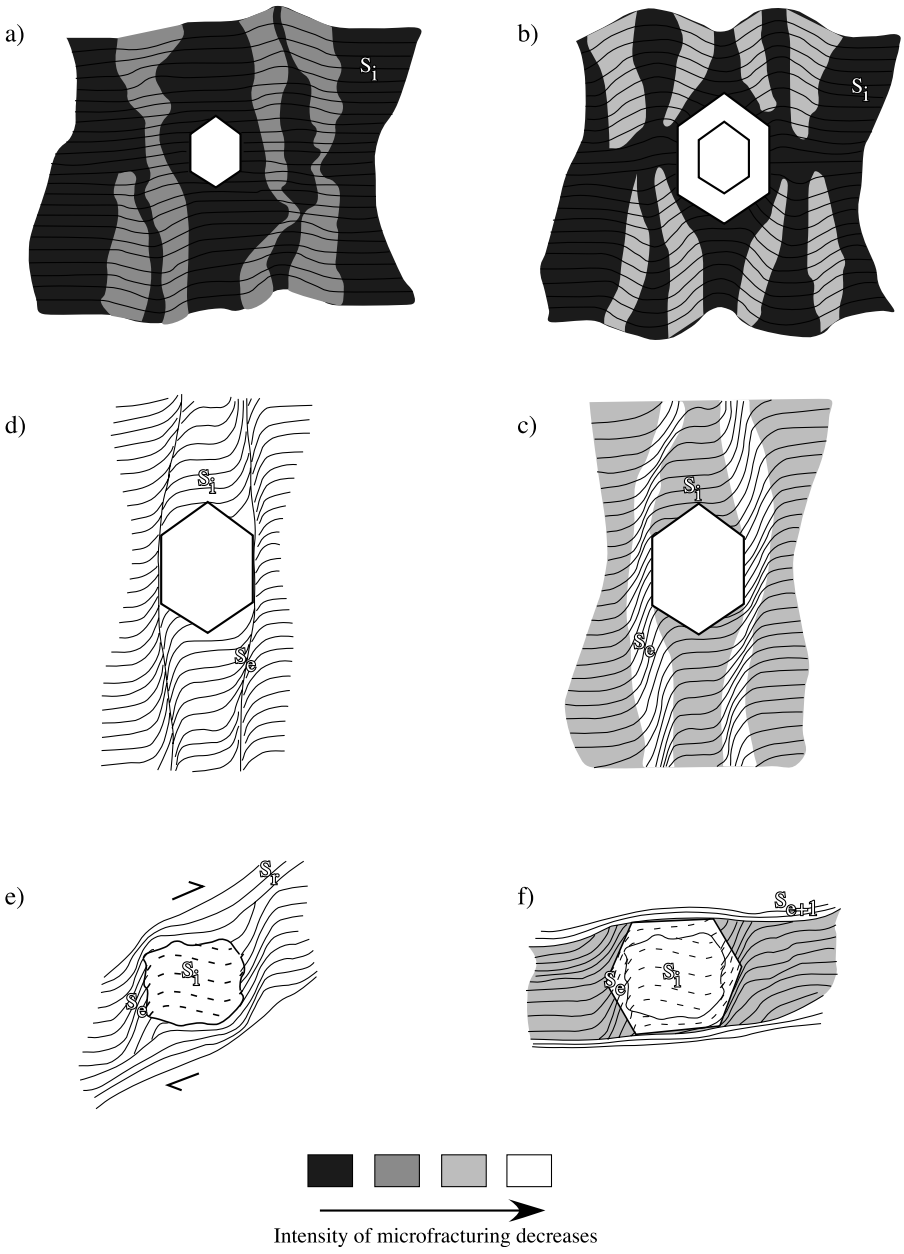

Fig. 15. A sketch figure showing the stages of porphyroblast growth and the effect of deformation partitioning from one event to another. Microfracture development occurs soon after the deformation commenced (a). As deformation continues the microfracture density decreases (b), and porphyroblast growth ceases once a differentiated crenulation cleavage is formed and a consistent pattern of deformation partitioning is achieved (c). As the deformation intensifies, micas recrystallize along progressive shearing domains (d). During later stages of the same deformation, S_e is destroyed and S_i is rotated towards the compositional layering because of the reactivation, hence S_r dominates the matrix but in the strain shadow of the porphyroblast S_e remains as a relict foliation (e). In the next deformation event, deformation is repartitioned and porphyroblast growth continues in the new progressive shortening sites (f). At this stage, relict S_e trapped as inclusions in the rim and S_{e+1} is formed in the matrix (modified from Bell et al. (2004)).

N–S and to NE–SW with time, and were contemporaneous with superimposed folding observed in the Georgetown Inlier (Fig. 1c). The lack of relationship between the asymmetry of inclusion trails for each FIA set and the macroscopic fold limbs suggests that the onset of folding in the area occurred before the growth of porphyroblasts and extensive metamorphism, possibly just after the depositional age of 1655 ± 2.2 Ma (Black et al., 1998).

The Northeast Australian Proterozoic basins including the Mt Isa, Georgetown, Coen, Yambo, Dargalong and Woolgar (Fig. 1) formed during rift related subsidence far away from the north-dipping subduction zone along the southern margin of the North Australian Craton between 1800 and 1650 Ma (O'Deal et al., 1997; Betts et al., 2002; Giles et al., 2002). It was suggested that this basin development was interrupted by Mesoproterozoic orogenesis (E–W shortening), which commenced along the eastern margin of the Australian Proterozoic continent at around

1600–1500 Ma because of convergence with North America (Betts et al., 2002). However, the evidence presented here reveals that deformation must have begun earlier sometime between 1655 and 1600 Ma, with NNW–SSE followed by N–S shortening. This suggests that longed-lived N–S subduction, which occurred between ca. 1800 and 1600 Ma, allowed transmission of compressive stresses to intra-continental settings (Scott et al., 2000) and caused regional E–W-trending folding. Then, deformation plus crustal thickening continued during E–W shortening and led to N–S-trending folding in the Georgetown Inlier, possibly as a result of convergence with North America. However, since both E–W and N–S folds (Bell, 1983; Page and Bell, 1986; Beardsmore et al., 1988; Connors and Page, 1995; Rubenach and Barker, 1998) as well as E–W and N–S FIAs (Mares, 1998) have been reported from the Mt Isa Inlier, these must be regional events that affected the bulk of the northern part of Australia. Finally, the last deformation episode that is characterized by NW–SE shortening might be associated with widespread granite intrusions occurred at around ca. 1550 Ma (e.g. Black et al., 1998).

7. Conclusions

(1) Detailed microstructural analysis and outcrop studies indicate that multiple deformation events predate the matrix foliations as currently preserved. These events are preserved as inclusion trails within porphyroblasts and have been totally destroyed and rotated by the reactivation of the bedding in the matrix.
(2) A succession of four FIA sets oriented, respectively, ENE–WSW, E–W, N–S and NE–SW were developed in the Robertson River Metamorphics. This FIA succession suggests that the bulk shortening direction shifted throughout deformation history from NNW–SSE to N–S to E–W and to NW–SE, which creates superimposed folding on a regional scale.
(3) The asymmetry of the inclusion trails examined on the limbs of the macro-scale folds showed that the folds predated porphyroblast growth and extensive metamorphism. This suggests that the onset of the folding must have occurred earlier than previously suggested at around ca. 1570 Ma. It is proposed here that this event must have commenced just after the depositional age of ca. 1655 Ma.
(4) Previously suggested progressive thin-skinned westward thrusting followed by thick-skinned E–W shortening tectonic model (e.g. Betts et al., 2002) for NE Australian Craton must be reconsidered.

Acknowledgements

I would like to thank Prof. Tim Bell for his valuable comments and improving the language of the manuscript. Thanks are also due to Drs Domingo Aerden, Aron Stallard and Prof. David Gray, whose reviews considerably improved an early version of the manuscript.

References

Aerden, D.G.A.M., 1995. Porphyroblast non-rotation during crustal extension in the Variscan Lys–Caillaouas Massif, Pyrenees. Journal of Structural Geology 17, 709–725.

Bain J.H.C., Withnall I.W., Oversby B.S., Mackenzie D.E., 1985. Geology of the Georgetown Region, Queensland. Australian Bureau of Mineral Resources Canberra, ACT, scale 1:250,000.

Beardsmore, T.J., Newbery, S.P., Laing, W.P., 1988. The Maronan Supergroup: an inferred early volcanosedimentary rift sequence in the Mt Isa Inlier, and its implications for ensialic rifting in the middle Proterozoic of Northwest Queensland. Precambrian Research 40/41, 487–507.

Bell, T.H., 1983. Thrusting and duplex formation at Mount Isa Queensland, Australia. Nature 304, 493–497.

Bell, T.H., 1986. Foliation development and refraction in metamorphic rocks: reactivation of earlier foliations and decrenulation due to shifting patterns of deformation partitioning. Journal of Metamorphic Geology 4, 421–444.

Bell, T.H., Rubenach, M.J., 1983. Sequential porphyroblast growth and crenulation cleavage development during progressive deformation. Tectonophysics 92, 171–194.

Bell, T.H., Fleming, P.D., Rubenach, M.J., 1986. Porphyroblast nucleation, growth and dissolution in regional metamorphic rocks as a function of deformation partitioning during foliation development. Journal of Metamorphic Geology 4, 37–67.

Bell, T.H., Forde, A., Wang, J., 1995. A new indicator of movement direction during orogenesis: measurement technique and application to the Alps. Terra Nova 7, 500–508.

Bell, T.H., Ham, A.P., Hickey, K.A., 2003. Early formed regional antiforms and synforms that fold younger matrix schistosities: their effect on sites of mineral growth. Tectonophysics 367, 253–278.

Bell, T.H., Ham, A.P., Kim, H.S., 2004. Partitioning of deformation along an orogen and its effects on porphyroblast growth during orogenesis. Journal of Structural Geology 26, 825–845.

Betts, P.G., Giles, D., Lister, G.S., Frick, L.R., 2002. Evolution of the Australian lithosphere. Australian Journal of Earth Sciences 49, 661–695.

Black, L.P., Bell, T.H., Rubenach, M.J., Withnall, I.W., 1979. Geochronology of discrete structural-metamorphic events in a multiply deformed Precambrian terrain. Tectonophysics 54, 103–137.

Black, L.P., Gregory, P., Withnall, I.W., Bain, J.H.C., 1998. U–Pb zircon age for the Etheridge Group, Georgetown region, north Queensland: implications for relationship with the Broken Hill and Mt Isa sequences. Australian Journal of Earth Sciences 45, 925–935.

Cihan, M., 2004. The drawbacks of sectioning rocks relative to fabric orientations in the matrix: a case study from the Robertson River Metamorphics (North Queensland, Australia). Journal of Structural Geology 26, 2157–2174.

Connors, K.A., Page, R.W., 1995. Relationships between magmatism, metamorphism and deformation in the western Mount Isa Inlier, Australia. Precambrian Research 71, 131–153.

Davis, B.K., 1996. Biotite porphyroblast nucleation and growth: control by microfracture of pre-existing foliations in schists in the Robertson River Metamorphics, Austalia. Geological Magazine 133, 91–102.

Giles, D., Betts, P., Lister, G., 2002. Far-field continental back-arc setting for the 1.80–1.67 Ga basins of northeastern Australia. Geological Society of America 30, 823–826.

Hayward, N., 1992. Microstructural analysis of the classical spiral garnet porphyroblasts of south-east Vermont: evidence for non-rotation. Journal of Metamorphic Geology 10, 567–587.

Hickey, K.A., Bell, T.H., 2001. Resolving complexities associated with timing macroscopic folds in multiply deformed terrains: the Spring Hill synform, Vermont. Bulletin of Geological Society of America 113, 1282–1298.

MacCready, T., Goleby, B.R., Goncharov, A., Drummond, B.J., Lister, G.S., 1998. A framework of overprinting orogens based on interpretation of the Mount Isa deep seismic transect. Economic Geology 93, 1422–1434.

Mares, V.M., 1998. Structural development of the Soldiers Cap Group in the Eastern Fold Belt of the Mt Isa Inlier: a succession of horizontal and vertical deformation events and large-scale shearing. Australian Journal of Earth Sciences 45, 373–387.

O'Dea, M.G., Lister, G.S., Betts, P.G., Pound, K.S., 1997. A shortened intraplate rift system in the Proterozoic Mt Isa terrain, NW Queensland, Australia. Tectonics 16, 425–441.

Page, R.W., Bell, T.H., 1986. Isotopic and structural responses of granite to successive deformation and metamorphism. Journal of Geology 94, 365–379.

Paterson, S.R., Vernon, R.H., 2001. Inclusion trail patterns in porphyroblasts from the Foothills Terrane, California; a record of orogenesis of local strain heterogeneity? Journal of Metamorphic Geology 19, 351–372.

Rosenfeld, J.L., 1970. Rotated garnets in metamorphic rocks. Geological Society of America Special Paper, 129.

Rubenach, M.J., Barker, A.J., 1998. Metamorphic and metasomatic evolution of the Snake Creek Anticline, Eastern Succession, Mt Isa Inlier. Australian Journal of Earth Sciences 45, 363–372.

Schonefeld, C., 1979. The geometry and significance of inclusion patterns in syntectonic porphyroblasts. Published PhD Thesis, University of Laiden, The Netherlands.

Scott, D.L., Rawlings, D.J., Page, R.W., Tarlowski, C.Z., Idnurm, M., Jackson, M.J., Southgate, P.N., 2000. Basement framework and geodynamic evolution of the Palaeproterozoic superbasins of north-central Australia: an integrated review of geochemical, geochronological and geophysical data. Australian Journal of Earth Sciences 47, 341–380.

Stallard, A., Hickey, K., 2001. Shear zone vs. folding origin for spiral inclusion trails in the Canton Schist. Journal of Structural Geology 23, 1845–1864.

Vernon, R.H., 1978. Porphyroblast-matrix microstructural relationships in deformed metamorphic rocks. Geologische Rundschau 68, 288–305.

Vernon, R.H., 1989. Porphyroblast-matrix microstructural relationships: recent approaches and problems. In: Daly, J.S., Cliff, R.A., Yardley, B.W. (Eds.), Evolution of Metamorphic Belts, vol. 43. Geological Society Special Publication, pp. 83–102.

Visser, P., Manctelow, N.S., 1992. The rotation of garnet porphyroblasts around a single fold, Lukmanier Pass, Central Alps. Journal of Structural Geology 14, 1193–1202.

White, D.A., 1965. The geology of the Georgetown/Clarke River area, Queensland. Australian Bureau of Mineral Resources Bulletin, 71.

Withnall, I.W., 1985. Geochemistry and tectonic significance of Proterozoic mafic rocks from the Georgetown Inlier, north Queensland. BMR Journal of Australian Geology and Geophysics 9, 339–351.

Withnall, I.W., 1996. Stratigraphy, structure and metamorphism of the Proterozoic Etheridge and Langlovale Groups, Georgetown region, north Queensland. Australian Geological Survey Organization Record, 1996/15.

Williams, M.L., 1994. Sigmoidal inclusion trails, punctuated fabric development, and interactions between metamorphism and deformation. Journal of Metamorphic Geology 12, 1–21.

Williams, P.F., 1985. Multiply deformed terrains – problems of correlation. Journal of Structural Geology 7, 269–280.

Zwart, H.J., 1960. The chronological succession of folding and metamorphism in the central Pyrenees. Geologische Rundschau 50, 203–218.